Results in Engineering 16 (2022) 100739

Contents lists available at ScienceDirect

Results in Engineering

journal homepage: www.sciencedirect.com/journal/results-in-engineering

Grain refinement of Al–Zn–Mg alloy during equal channel angular pressing (ECAP)

Oryina Mbaadega Injor [a], Oluyemi Ojo Daramola [a,**], Benjamin Omotayo Adewuyi [a], Adeolu Adesoji Adediran [b,f,*], Munyadziwa Mercy Ramakokovhu [c], Rotimi Emmanuel Sadiku [d], Esther Titilayo Akinlabi [e]

[a] Department of Metallurgical and Materials Engineering, Federal University of Technology, Akure, 340001, Nigeria
[b] Department of Mechanical Engineering, Landmark University, Omu-Aran, Kwara State, Nigeria
[c] Institute of NanoEngineering Research, Department of Chemical, Metallurgical and Materials Engineering, Tshwane University of Technology, Pretoria, South Africa
[d] Institute of NanoEngineering Research, Department of Chemical, Metallurgical and Materials Engineering, Polymer Division, Tshwane University of Technology, Pretoria, South Africa
[e] Department of Mechanical and Construction Engineering, Faculty of Engineering and Environment, Northumbria University, Newcastle, UK
[f] Department of Mechanical Engineering Science, University of Johannesburg, South Africa

A R T I C L E I N F O

Keywords:
Equal channel angular pressing
Severe plastic deformation
Aluminum alloy

A B S T R A C T

Locally produced Al–Zn–Mg alloy was subjected to severe plastic deformation through Equal Channel Angular Pressing (ECAP) technique at temperatures of 150 °C and 200 °C. Rectangular thick-walled medium carbon steel die (σ_c = 450Mpa, σ_y = 176Mpa) with an L-shaped channel of uniform configuration to provide the pressing chamber was used. Four ECAP passes were imposed consecutively on set of samples for 150 °C and 200 °C temperatures, and characterized with optical microscopy, scanning electron microscopy (SEM) and x-ray diffraction (XRD). The phases were identified by X-ray diffraction (XRD) using monochromatic Cu Kα radiation, while vickers' microhardness and tensile tests were performed for mechanical properties examination. Optical micrographs showed no tangible precipitation in the as cast samples with reduced grain width and deformation bands but at high temperatures of 150 °C and 200 °C, precipitation was promoted as a result of slipping systems activation. SEM images of the as-cast alloy exhibits dendrites of 250 ± 20 μm in size with η′ phase ($MgZn_2$) precipitates in the inter-dendritic regions. For 150 °C ECAP temperature, a significant refinement was achieved as the passes increased with sub-grain development within the boundary and the precipitate observed has a grain size of 35 ± 15 μm, 25 ± 10 μm, 15 ± 8 μm and 8 ± 6 μm for first, second, third and fourth passes respectively. However, grain sizes of 85 ± 15 μm, 50 ± 10 μm, 30 ± 8 μm and 10 ± 5 μm for first, second, third and fourth passes were observed for 200 °C ECAP temperature. XRD results showed peaks for aluminum and other phases in as-cast condition with precipitates growth in the alloy after the first pass, identified as metastable η' phase. As the number of ECAP passes increases, η' peaks moved towards the equilibrium η phase confirming the transformation of η' phase to stable η phase. The microhardness, Ultimate tensile strength (UTS) and the yield strength of Al–Zn–Mg alloy in different conditions of 150 °C and 200 °C respectively also increased with increase in the number of ECAP passes. This is due to increase in dislocation density, work hardening and grain refinement during ECAP process.

1. Introduction

In the contemporary age, the most crucial challenge is to improve the physical and mechanical properties of materials, exclusively for metals and their alloys [1]. One of the principal tools for controlling the mechanical properties of metallic materials is the grain size of a polycrystalline material [2,3]. Under deformation conditions when resistance to plastic flow is governed by dislocation glide, a reduction in the grain size leads to the strengthening of the material. The technique to get alloys with ultrafine grains during severe plastic deformation comprises

* Corresponding author. Department of Mechanical Engineering, Landmark University, Omu-Aran, Kwara State, Nigeria.
** Corresponding author. Department of Metallurgical and Materials Engineering, Federal University of Technology, Akure, Nigeria.
E-mail addresses: oodaramola@futa.edu.ng (O.O. Daramola), adediran.adeolu@lmu.edu.ng (A.A. Adediran).

https://doi.org/10.1016/j.rineng.2022.100739
Received 26 July 2022; Received in revised form 27 October 2022; Accepted 28 October 2022
Available online 4 November 2022

any procedure that, after subjecting a material to excessive stress (hydrostatic pressure), results to a significant plastic deformation without a substantial change to its dimensions [4].

Conventional metal forming procedures, such as extrusion or rolling, have a limited ability to produce ultra-fine grain (UFG) structures because the overall strain imposed is limited and insufficient to give rise to UFG structures because of the generally low workability of metallic alloys at ambient temperatures. Other traditional methods, such as rapid solidification and vapor condensation, are capable of refining materials down to the nanoscale, but these methods are limited to thin layers only. As a result of these restrictions, there is a paradigm shift on synthetic pathways for nanoscale materials and alternative processing techniques have developed. The severe plastic deformation (SPD) technique is one of such process, where extremely high strains are imposed at relatively low temperatures. It is a ground-breaking process for transforming bulk materials into ultrafine-grained structure with remarkable flexibility and strength [5]. Over the past two decades, SPD has become a well-known process for grain refinement of metals and alloys in the submicron or even nanometer range. The synthesis of UFG materials by SPD refers to several experimental metal forming processes that can be used to induce very high strains on materials, resulting in exceptional grain refinement. Equal Channel Angular Pressing (ECAP) is accepted as the most prevalent bulk severe plastic deformation processing technique and has been employed for the grain refinement in some metals and alloys [6]. It is a well-known SPD process for producing UFG bulk materials with equiaxed microstructure and high-angle grain boundary misorientation, discloses the improvement in mechanical properties such as yield strength, ultimate tensile strength and microhardness after a number of passes [7–9]. It is a metal forming process that induces intense plastic strain in the specimen without changing the cross-sectional area, and allowing the specimen to be repeatedly processed to exhibit high plastic strain [10]. ECAP is very easy to perform compared to other processes leading to nanostructured materials due to process simplicity, tooling and low cost. This process allows a metal or alloy to undergo SPD, which breaks down the original texture into ultrafine or even nanostructured material. After several passes, high strain is imposed on the sample, introducing a high density of dislocations, which in turn rearrange to form high-angle grain boundaries [11–15]. The most suitable material for the ECAP process is aluminum and its alloys, but heat treatable alloys typically fail by cracking due to the difficulty of processing at room temperature, resulting in loss of material deformation as a result of the formation of precipitates in solution-treated aluminum alloys [16–21]. Age-hardenable aluminum alloys, despite this difficulty, find applications in the aerospace industry and the ECAP process of these alloys is becoming popular every day, combining a nanocrystalline microstructure with precipitation hardening [20,22–25]. A strategy has been developed to process these alloys at an ambient temperature of ECAP, and it has been found that it can be pressed without cracking when performed immediately after quenching from the treatment temperature of the solution [21,26]. These alloys can be processed in over aged condition [27]. In addition, the precipitation microstructure of the age-hardenable Al alloy is very complicated by the ECAP process. At room temperature, precipitation in quenched samples is suppressed during the ECAP process, leading to dissolution and fragmentation of pre-existing phases [24,28]. The precipitation process and the suppression of some phases during the heat treatment can also be influenced by the ECAP process [29]. At high temperature, there are changes in precipitation kinetics and precipitation morphology are promoted by the ECAP process [20,24,30]. It has been shown that the process of ECAP in the alloy Al7034 to 473 K imposed with a high stress resulting from the fragmentation of the $MgZn_2$ precipitates, and a uniform distribution of fine spherical precipitates is generated [30,31]. This precipitated microstructure results in structural stability at temperatures up to 673 K [30–32]. Al–Zn–Mg alloy have high strength and a high content of alloying elements. While there is little information in the literature on the effect of the ECAP process in this alloy [33,34], further strengthening of other hardening mechanisms, such as the solid solution, grain refinement, the strengthening of the dislocation and the precipitation hardening, takes place during the ECAP process. The effect of these mechanisms is subject to the initial state of the alloy. The ECAP generally can lead to a remarkable improvement in strength compared to the alloy processed by other methods [35].

The aim of this work is to investigate the effect of ECAP process on the grain refinement of the high strength locally produced Al–Zn–Mg alloy. The influence of ECAP process on the grain structure, precipitation and mechanical properties are discussed for better understanding of high strength Al–Zn–Mg alloy behavior during ECAP process.

2. Experimental procedure

Rectangular shaped cast samples of Al–Zn–Mg alloy with dimension $(20 \times 20 \times 280)\ mm^3$ were turned and machined to produce the desired samples with dimension $(15 \times 15 \times 90)\ mm^3$ for ECAP pressing [36]. The chemical composition of the cast alloy was obtained using Atomic Absorption Spectrometry (AAS) as shown in Table 1. The ECAP die was locally fabricated from a rectangular thick-walled steel with dimension $(100 \times 100 \times 200)\ mm^3$. An L-shaped channel of uniform configuration was made on one of the split parts with dimension $(15 \times 15 \times 230)\ mm^3$ using AJAX 1 milling machine to provide the pressing chamber. The ECAP die had an internal angle of 90° and an additional angle of 20° at the outer radius of concordance where the two channels intersect. The schematic diagram of the ECAP die is shown in Fig. 1.

The heating of die and samples to 150 °C and 200 °C was done using heating elements integrated to the die, while a thermocouple inserted in the die located very close to the intersection of the channels controlled the temperature The pressing was done by route Bc, in which the sample undergo rotation between the passes. A punch/ram was machined with dimension $(14 \times 14 \times 250)\ mm^3$ for pressing of samples into the channel under high pressure. The machined samples were initially preheated to a temperature of 500 °C and kept constant at that temperature for 30 min for the purpose of stress relief of the samples using temperature control of resistance digital electric furnace with Model NYC 20. After preheating, the samples were lubricated with molybdenum-based lubricant (Filtex) and loaded into the ECAP-Die with the ram inserted and the loading of the sample was completed, ready for pressing. The pressing was done using ELE Compact-1500 hydraulic compression testing machine at 2 mm/s using standard route Bc in which the sample undergo rotation between the passes. A total of 32 samples were pressed using 150 °C temperature condition while another 32 samples were pressed using 200 °C temperature condition and 8 samples were used as control and not subjected to ECAP. Samples were identified by letter P followed by a digit indicating the ECAP pass number.

Microstructure of samples after ECAP process was done by optical microscopy (OM) and scanning electron microscopy (SEM). Samples for OM and SEM were prepared conventionally by metallographic preparation. Optical microscope with model- Olympus DP72 with computerized imaging system was used to view the samples at 50 μm magnifications. Scanning electron microscopy (SEM) investigations were carried out on a scanning electron microscope model- Zeiss 540 ultra, equipped with energy-dispersive spectrometer (EDS), and average grain size was evaluated using imageJ software. X-ray diffractometer (XRD) with model- RAYONS X was used to analyze and view the various phases present in the Al–Zn–Mg alloy. This was done using D/max- 250 x-ray diffractometer with Cu-Kα radiation of 1.54 Å at 30 kV tube voltage and a current of 20 mA and a scanning speed of 1°/min. The crystal structures and their peak intensities were identified using X'Pert Highscore Plus software. Vickers method was used to determine the microhardness of specimen with dimensions 15 $mm \times 15$ mm according to ASTM E−834 using microhardness tester with model FM-800 where the applied load of 50 gm for 15 s dwell time was imposed on samples. Four measurements were taken from each sample and the average value was recorded.

Table 1
Chemical composition of Al–Mg–Zn alloy.

Element	Si	Fe	Cu	Mn	Mg	Cr	Ni	Zn	B	Be
Chemical Composition (%)	0.82	0.16	1.87	0.183	2.66	0.0194	0.102	5.79	0.0014	0.00046
Element	Bi	Ca	Co	Na	Pb	Sn	Zr	Al		
Chemical Composition (%)	0.0035	0.0012	0.00061	0.00014	0.0505	0.0292	0.0029	Base		

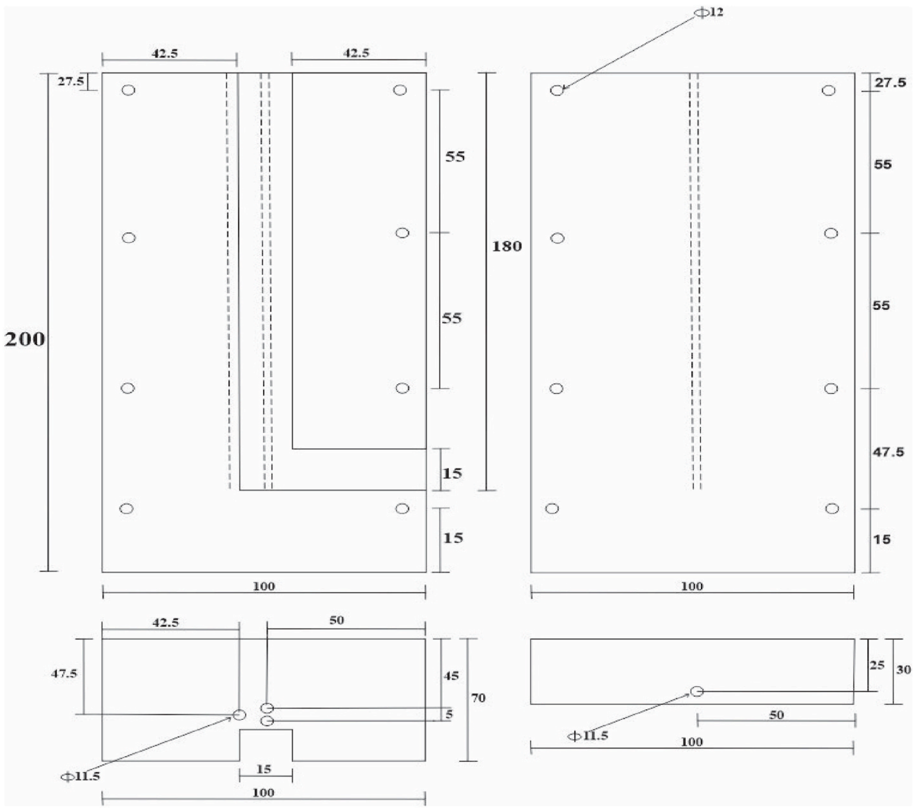

Fig. 1. Schematic diagram of the ECAP die.

Tensile strength testing of all specimens was conducted as per ASTM E8 standard. Tensile samples with dimensions of 50 mm gauge length, 12.5 mm width and 15 mm grip section thickness were machined using EXCEL 14402 model lathe machine. Four identical tests specimen per sample were tested at room temperature with a strain/loading rate of 5 mm/min using a computerized Instron Testing Machine with model-3369. Four samples of each condition were tested and load displacement plots were obtained and ultimate tensile strength and yield strength values were also obtained from the machine.

3. Results and discussion

The microstructural display of samples of Al–Zn–Mg alloy produced before and after ECAP process at 150 °C and 200 °C respectively is shown in Figs. 2 and 3 respectively.

From the results, it was observed that there was no tangible precipitation in the as cast samples with reduced grain width and deformation bands (Fig. 2a). But when the process was carried out at high temperatures (150 °C and 200 °C), precipitation was promoted which may be attributed to activation of more slipping systems at higher temperature. Samples after ECAP process at 150 °C has a high density of precipitates particles even after the first pass ($P_1$150) (Fig. 2 b-e). This agrees with Sha et al. [37] who reported that ECAP in Al–Zn–Mg–Cu alloy performed at 200 °C from a solubilized condition accelerates the precipitation rate while the change in the expected precipitation sequence for conventional ageing treatment (GP zones→ $\eta' \rightarrow \eta$) remains constant. As the number of ECAP passes increased from $P_1$200 to $P_4$200, the deformation bands became more homogeneously distributed and the resulting microstructure became more refined (Fig. 3a–d). The microstructure evolved into a fine equiaxial grain structure, which may also be attributed to different slip planes that are activated with the rotation of the sample thereby producing potentials for grain refinement using route Bc [38,39].

Fig. 4 showed the SEM micrographs of Al–Zn–Mg alloy processed at 150 °C temperature condition.

The microstructure of the as-cast alloy exhibits the characteristic feature of dendrites 250 ± 20 μm in size as shown in Fig. 4a. In addition, η′ phase ($MgZn_2$) precipitates were noted in the interdendritic regions [40]. A significant amount of refinement was achieved in $P_1$150 as shown in Fig. 4b, and sub-grain boundaries were developed within the grains with few elongated grains. Precipitates were observed near the grain boundaries with a grain size of 35 ± 15 μm. Fig. 4c displayed the microstructure of the alloy after $P_2$150. A grain size of 25 ± 10 μm was observed in this condition, similar in shape to that which was observed in the alloy after $P_1$150. Fig. 4d showed that shear bands were developed within the grains and sub-grains after $P_3$150 and these shear bands were 15 ± 8 μm in width. Fig. 3e showed the microstructure of the alloy after $P_4$150. Shear bands were seen in this condition to be more numerous with 8 ± 6 μm in width.

Fig. 5 illustrates the SEM micrographs of Al–Zn–Mg alloy processed

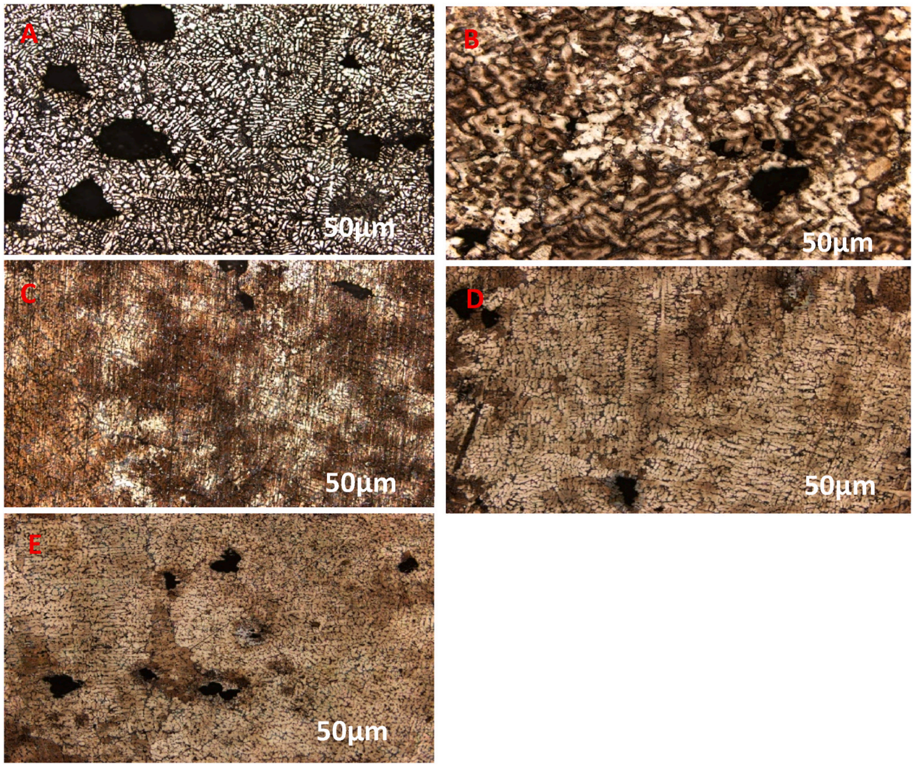

Fig. 2. Optical micrographs of Al–Zn–Mg alloy; (a) P_0 (b) $P_1$150 (c) $P_2$150 (d) $P_3$150 (e) $P_4$150.

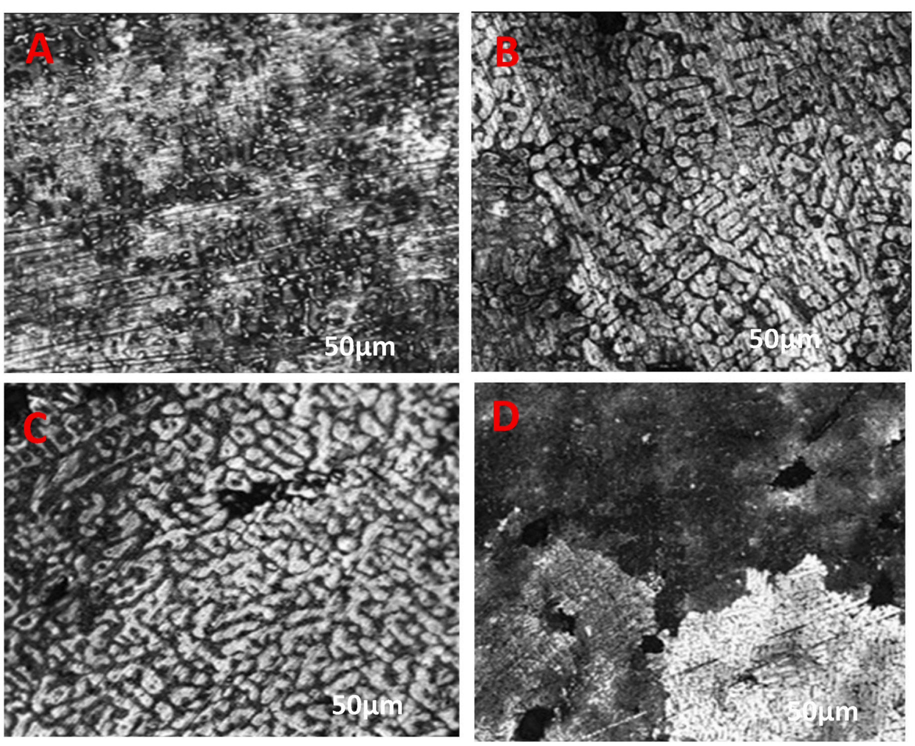

Fig. 3. Optical micrographs of Al–Zn–Mg alloy; (a) $P_1$200 (b) $P_2$200 (c) $P_3$200 (d) $P_4$200.

at 200 °C temperature condition.

After $P_1$200, grain structure was significantly refined as shown in Fig. 5a with a grain size of 85 ± 15 μm observed due to the development of sub-grain boundaries inside the grains with precipitate developed near the grain boundaries. Fig. 5b shows the microstructure of the alloy after $P_2$200 and a grain size of 50 ± 10 μm was observed in this condition. Fig. 5c showed that shear bands were developed within the grains and sub-grains after $P_3$200 and these shear bands were 30 ± 8 μm in width. Fig. 5d shows the microstructure of the alloy after $P_4$200, where shear bands were perceived in this condition to be more with

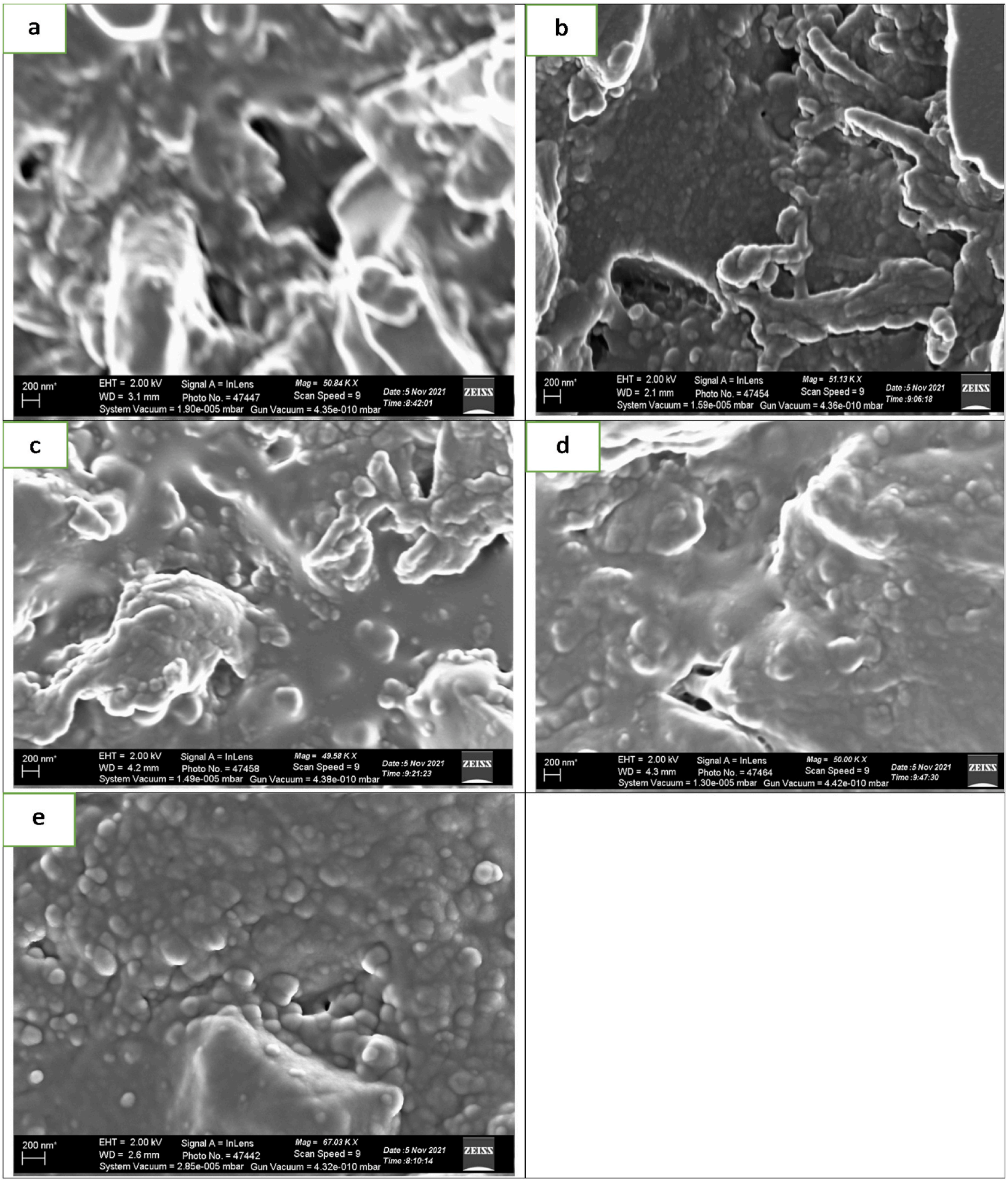

Fig. 4. Sem micrographs of Al–Zn–Mg alloy for (a) P_0 (b) P_1150 (c) P_2150 (d) P_3150 (e) P_4150.

dimension of 10 ± 5 μm in width.

In comparison to Al–Zn–Mg alloy processed at 150 °C, the quantity of precipitates developed in Al–Zn–Mg alloy processed at 200 °C after ECAP is lower due to the temperature difference. Both conditions showed equiaxed and homogeneous microstructure in P_3 and P_4.

X-ray diffractometry was used to determine the crystallographic structure of the alloy produced both before and after ECAP process for 150 °C and 200 °C temperature conditions respectively as shown in Figs. 6 and 7.

From the results it was found that there were peaks for aluminum and other phases in as-cast condition. Those peaks correspond to intermetallic hexagonal η' ($MgZn_2$) phase and the lattice parameter of these peaks was slightly bigger than equilibrium η ($MgZn_2$) phase [41–43]. In the conventional sequence Al–Zn–Mg alloys form precipitates starting from the solid solution to GP zones followed by metastable precipitate η' and then equilibrium phase η ($MgZn_2$). For ECAP processed at 150 °C under various conditions, it was observed that there were peaks for aluminum and other phases corresponding to metastable η' ($MgZn_2$) phase precipitates. This is because, the dislocations generated during ECAP processing act as nucleation sites for the development of the precipitates [44]. Hence, precipitate growth was observed after first pass. As the number of ECAP passes increases, η' peaks moved towards the equilibrium η phase confirming the transformation of η' phase to stable η phase [41]. For 200 °C ECAP processed samples, XRD plots were similar to those observed in the same alloy ECAP processed at 150 °C. Peaks of the aluminium and other small peaks related to η' phase

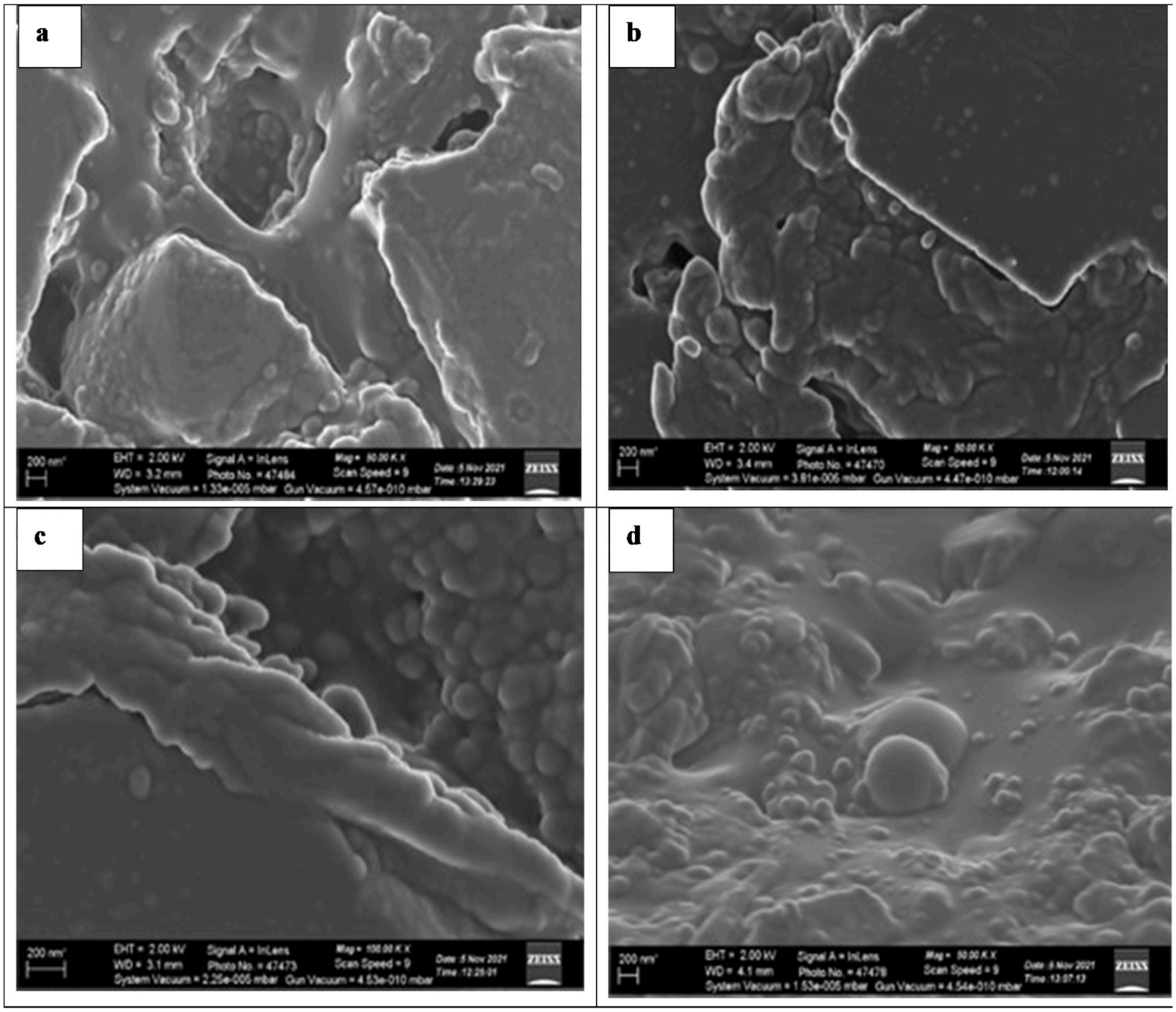

Fig. 5. Sem micrographs of Al–Zn–Mg alloy for (a) P_1200 (b) P_2200 (c) P_3200 (d) P_4200.

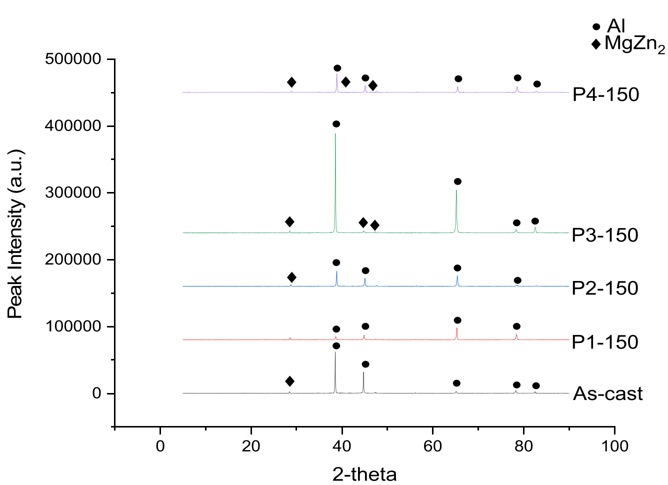

Fig. 6. The X-ray diffraction patterns on the cross-sections of samples after ECAP at 150 °C temperature condition.

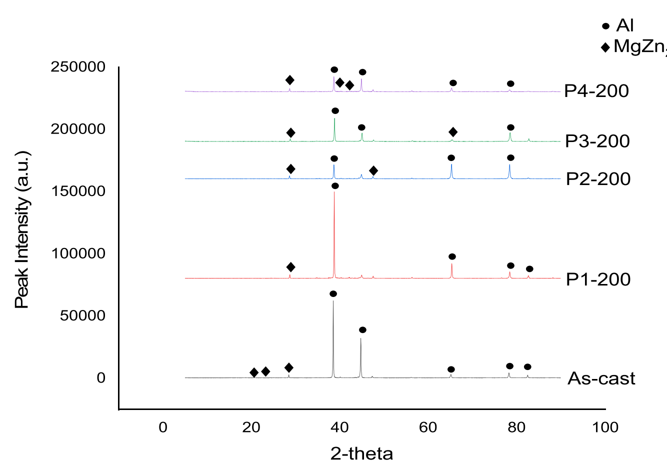

Fig. 7. The X-ray diffraction patterns on the cross-sections of samples after ECAP at 200 °C temperature condition.

precipitates were observed after first pass. Also, with increase in the number of ECAP passes there was transformation of η′ phase to stable η phase as the η′ peaks move towards η phase.

The effect of Al–Zn–Mg ally processed by ECAP technique on hardness for 150 °C and 200 °C temperature conditions is shown in Fig. 8.

It was observed that there was increase in the microhardness of the alloy with decrease in the grain size. For P_0, the microhardness was 123 Hv, thereafter there was notable improvement in the microharhness after ECAP processing. The microhardness of the alloy was improved to 151 Hv for P_1150 and 127 Hv for P_1200, 203 Hv for P_2150 and 147 Hv for P_2200, 219 Hv for P_3150 and 166 Hv for P_3200 and 224 Hv for P_4150

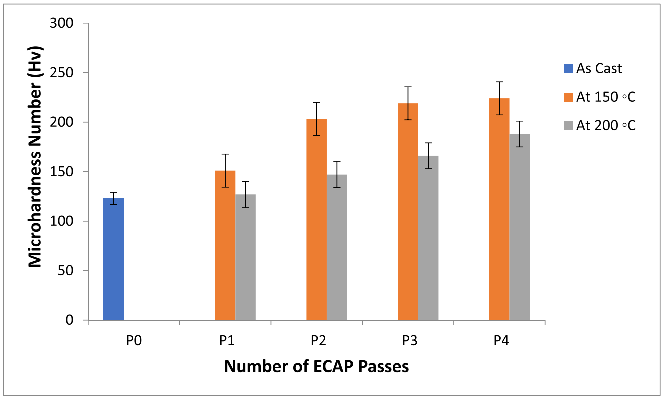

Fig. 8. Plot of microhardness against the number of ECAP passes.

and 188 Hv for $P_4$200 respectively.

This increase in hardness, at 150 °C and 200 °C ECAP processing temperatures results from precipitation, work hardening and microstructure refinement due to high dislocation density developed during ECAP processing and also the development of fine and elongated grain structure with deformation bands present in some grains interior that was distributed homogenously in the alloy [41]. Deformation bands are formed because it is not difficult for a constrained grain to deform by splitting into bands [39,45]. This new high angle grain boundary formation induced by deformation can occur if there is increase in the misorientation between the deformation bands [41].

The effect of Al–Zn–Mg alloy produced by ECAP technique on tensile and yield strength for 150 °C and 200 °C temperature conditions is shown in Figs. 9 and 10 respectively.

It was observed that the Ultimate tensile strength (UTS) and the yield strength (YS) of Al–Zn–Mg alloy in different conditions of 150 °C and 200 °C respectively increased with increase in the number of ECAP passes. For P_0, the UTS of the alloy was 200.22 MPa with a yield strength of 146.12 MPa. ECAP processing leads to a drastic improvement in the strength of the material. After ECAP processing at 150 °C, the UTS of the alloy increased from 293.56 MPa for $P_1$150, 318.08 MPa for $P_2$150, 437.08 MPa for $P_3$150 and 491.06 MPa for $P_4$150 respectively with corresponding increase in the yield strength from 266.16 MPa for $P_1$150 to 468.61 MPa for $P_4$150. The same trend was also observed for ECAP process at 200 °C where the UTS increased from 236.18 MPa for $P_1$200 to 339.12 MPa for $P_4$200 respectively with equivalent increase in the yield strength. The increase in yield strength is credited to increase in dislocation density, work hardening and grain refinement during ECAP process described by Hall-Petch equation which states that the yield strength is inversely proportional to the average grain size of the material [46]. The summary of the obtained results on the mechanical properties is presented in Table 2.

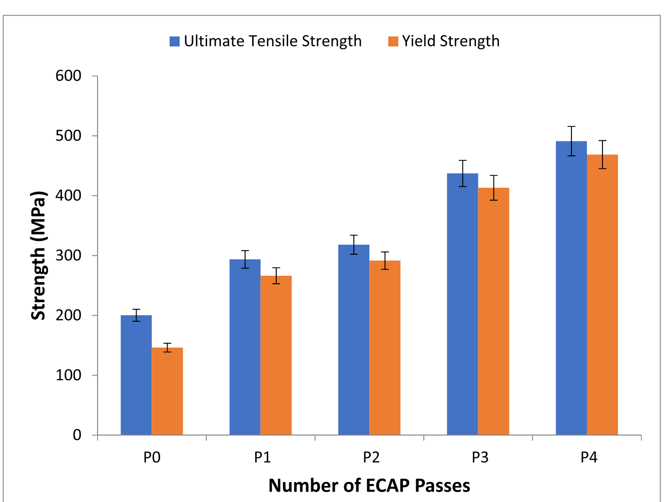

Fig. 9. Plot of tensile and yield strength against the number of ECAP passes at 150 °C temperature condition.

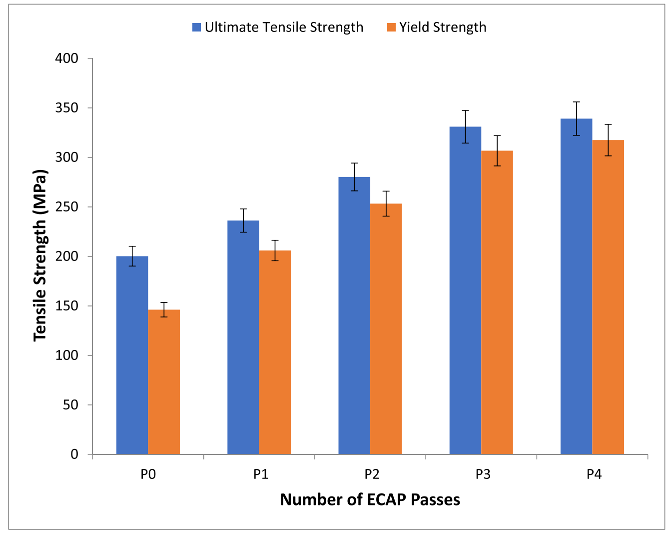

Fig. 10. Plot of tensile and yield strength against the number of ECAP passes at 200 °C temperature condition.

4. Conclusion

Locally produced Al–Zn–Mg alloy was successfully processed using Equal Channel Angular Pressing (ECAP) technique at 150 °C and 200 °C respectively.

Optical microscopy showed that the quantity of precipitates developed in Al–Zn–Mg alloy processed at 150 °C after ECAP is higher than the ones developed at 200 °C and both conditions showed equiaxed and homogeneous microstructure as the number of passes increased. There was no tangible precipitation in the as cast samples but precipitation was promoted at 150 °C and 200 °C because of activation of more slipping systems at higher temperatures.

SEM images of the as-cast alloy (P_0) exhibits dendrites of 250 ± 20 μm in size with η′ phase ($MgZn_2$) precipitates in the inter-dendritic regions, while there is significant refinement as the number of passes increased with sub-grain development within the boundary with precipitates developed near the grain boundaries for both 150 °C and 200 °C ECAP temperatures. For 150 °C the grain refinement ranges from 35 ± 15 μm to 8 ± 6 μm for $P_1$150 to $P_4$150 while for 200 °C the grain refinement ranges from 85 ± 15 μm to 10 ± 5 μm for $P_1$200 to $P_4$200.

The XRD crystallographic structure showed peaks for aluminum and other phases in as cast condition revealing peaks corresponding to intermetallic hexagonal η' ($MgZn_2$) phase with lattice parameter slightly bigger than equilibrium η ($MgZn_2$) phase. As the number of ECAP passes increases for both 150 °C and 200 °C ECAP temperatures, η' peaks moved towards the equilibrium η phase confirming the transformation of η' phase to stable η phase.

The ultimate tensile strength and yield strength of Al–Zn–Mg alloy in different conditions of 150 °C and 200 °C increased with increase in the number of ECAP passes. For 150 °C the highest tensile strength was 491.06 MPa with 486.61 MPa yield strength, while at 200 °C the highest tensile strength was 339.12 MPa with 317.47 MPa yield strength.

There was increase in hardness at 150 °C and 200 °C because of microstructure refinement due to high dislocation density with fine and elongated grain structure developed during ECAP processing.

Generally, the properties of the alloy processed at 150 °C were better

Table 2
Summary of the mechanical properties of ECAPed Al–Zn–Mg alloy at various passes and temperatures.

ECAP PASSES									
MECHANICAL PROPERTIES	P_O	$P_1$150	$P_2$150	$P_3$150	$P_4$150	$P_1$200	$P_2$200	$P_3$200	$P_4$200
Hardness (Hv)	123	151	203	219	224	127	147	166	188
UTS (mPa)	200.22	293.56	318.08	437.08	491.08	236.18	280.26	330.96	339.12
YS (mPa)	146.12	266.16	291.44	413.13	468.61	205.97	253.27	306.75	316.47

than those processed at 200 °C because at higher temperatures, there is degradation of strength by dislocation or coarsening of the strengthening precipitates.

Credit author statement

Benjamin Omotayo Adewuyi, Oluyemi Ojo Daramola: Conceptualization, Methodology, Software Oryina Mbaadega Injor, Oluyemi Ojo Daramola, Benjamin Omotayo Adewuyi.: Data curation, Writing – original draft. Oryina Mbaadega Injor: Visualization, Investigation. Oluyemi Ojo Daramola, Benjamin Omotayo Adewuyi: Supervision: Adeolu Adesoji Adediran, Munyadziwa Mercy Ramakokovhu, Rotimi Emmanuel Sadiku, Esther Titilayo Akinlabi: Software, Validation.: Oryina Mbaadega Injor, Oluyemi Ojo Daramola, Benjamin Omotayo Adewuyi, Adeolu Adesoji Adediran, Munyadziwa Mercy Ramakokovhu, Rotimi Emmanduel Sadiku, Esther Titilayo Akinlabi: Writing- Reviewing and Editing.

Declaration of competing interest

The authors declare that they have no known competing financial interests or personal relationships that could have appeared to influence the work reported in this paper.

Data availability

No data was used for the research described in the article.

References

[1] S.K. Mohapatra, V. Rajan, S. Tripathy, Study of severe plastic deformation of metallic materials: a move towards amorphization, Mater. Today Proc. (2022) 735–741.
[2] E.O. Hall, The deformation and ageing of mild steel: III discussion of results, Proc. Phys. Soc. B 64 (1951) 747–753.
[3] N.J. Petch, The cleavage strength of polycrystals, Iron Steel Inst 174 (1953) 25–28.
[4] F.D. Carazo, J.J. Pastor Alés, J. Signorelli, D.J. Celentano, C.M. Guevara, R. Lucci, Analysis of strain inhomogeneity in extruded Al 6060-T6 processed by ECAE, Metals 12 (299) (2022) 1–15.
[5] A. Awasthi, U.S. Rao, K.K. Saxena, R.K. Dwivedi, Impact of equal channel angular pressing on aluminum alloys: an overview, Mater. Today Proc. 57 (2) (2022) 908–912.
[6] B. Mishra, S.K. Mohapatra, V. Rajan, K. Maity, Equal channel angular pressing of aluminum alloy: a numerical investigation, Mater. Today Proc. 26 (2) (2020) 2173–2178, 8.
[7] R.Z. Valiev, T.G. Langdon, Principles of equal-channel angular pressing as a processing tool for grain refinement, Prog. Mater. Sci. 51 (7) (2006) 881–981.
[8] H.K. Govindaraju, S.M. Kumar, M.D. Kiran, Fracture analysis and tensile properties of ECAP Al-Zn alloy for industrial application, J. Fail. Anal. Prev. 21 (2021) 1784–1794.
[9] M. Chegini, M. Shaeri, Effect of equal channel angular pressing on the mechanical and tribological behavior of Al-Zn-Mg-Cu alloy, Mater. Char. 140 (2018) 147–161.
[10] Y.T. Zehetbauer, M.J. Zhu, Bulk Nanostructured Materials, Wiley-VCH, Weinheim, 2009.
[11] R.Z. Valiev, Nanostructuring of metals by severe plastic deformation for advanced properties, Nat. Mater. 3 (2004) 511–516.
[12] R.Z. Valiev, T.G. Langdon, Principles of equal-channel angular pressing as a processing tool for grain refinement, Prog. Mater. Sci. 51 (7) (2006) 881–981.
[13] V.M. Segal, Materials processing by simple shear, Mater. Sci. Eng. 197 (2) (1995) 157–164.
[14] Y. Iwahashi, J. Wang, Z. Horita, M. Nemoto, T.G. Langdon, Principle of equal-Channel Angular pressing for the processing of ultra-fine grained materials, Scripta Mater. 35 (1996) 143–146.
[15] F. Djavanroodi, M. Ebrahimi, Effect of die channel angle, friction and back pressure in the equal channel angular pressing using 3D finite element simulation, Mater. Sci. Eng. 527 (2010) 1230–1235.
[16] A. Gholinia, P.B. Prangnell, M.V. Markushev, The effect of strain path on the development of deformation structures in severely deformed aluminum alloys processed by ECAE, Acta Mater. 48 (5) (2000) 1115–1130.
[17] M. Furukawa, Z. Horita, T.G. Langdon, Processing by equal-Channel Angular pressing: applications to grain boundary engineering, J. Mater. Sci. 40 (2005) 909–917.
[18] Y. Iwahashi, Z. Horita, M. Nemoto, T.G. Langdon, An investigation of microstructural evolution during equal-Channel Angular pressing, Acta Mater. 45 (1997) 4733–4741.
[19] N.Q. Chinh, J. Gubicza, T. Czeppe, J. Lendvai, C. Xu, R.Z. Valiev, et al., Developing a strategy for the processing of age-hardenable alloys by ECAP at room temperature, Mater. Sci. Eng. 516 (2009) 248–252.
[20] J. Gubicza, I. Schiler, N.Q. Chinh, J. Illy, Z. Horita, T.G. Langdon, The effect of severe plastic deformation on precipitation in supersaturated Al-Zn-Mg alloys, Mater. Sci. Eng. 460–461 (2007) 77–85.
[21] M.R. Roshan, S.A. Jenabali Jahromi, R. Ebrahimi, Predicting the critical pre-aging time in ECAP processing of age-hardenable aluminum alloys, J. Alloys Compd. 509 (2011) 7833–7839.
[22] S. Dadbakhsh, A. Karimi Taheri, C.W. Smith, Strengthening study on 6082 Al alloy after combination of aging treatment and ECAP process, Mater. Sci. Eng. 527 (18–19) (2010) 4758–4766.
[23] Y.H. Zhao, X.Z. Liao, Z. Jin, R.Z. Valiev, Y.T. Zhu, Microstructures and mechanical properties of ultrafine grained 7075 Al alloy processed by ECAP and their evolutions during annealing, Acta Mater. 52 (2004) 4589–4599.
[24] G. Sha, Y.B. Wang, X.Z. Liao, Z.C. Duan, S.P. Ringer, T.G. Langdon, Influence of equal-Channel Angular pressing on precipitation in an Al-Zn-Mg-Cu alloy, Acta Mater. 57 (2009) 3123–3132.
[25] T. Radetic, M. Popovic, E. Romhanji, B. Velinden, The effect of ECAP and Cu addition on the aging response and grain substructure evolution in an Al-4.4 wt.% Mg alloy, Mater. Sci. Eng. 527 (3) (2010) 634–644.
[26] Z.C. Duan, N.Q. Chinh, C. Xu, T.G. Langdon, Developing processing routes for the equal-channel angular pressing of age-hardenable aluminum alloys, Metall. Mater. Trans. 41A (8) (2010) 802–809.
[27] C.M. Cepeda-Jiménez, J.M. García-Infanta, O.A. Ruano, F. Carreño, Mechanical properties at room temperature of an Al-Zn-Mg-Cu alloy processed by equal channel angular pressing, J. Alloys Compd. 509 (35) (2011) 8649–8656.
[28] Z. Liu, S. Bai, X. Zhou, Y. Gu, On strain-induced dissolution of θ'and θ particles in Al-Cu binary alloy during equal channel angular pressing, Mater. Sci. Eng. 528 (2011) 2217–2222.
[29] M. Murayama, Z. Horita, K. Hono, Microstructure of two-phase Al-1.7 at% Cu alloy deformed by equal-channel angular pressing, Acta Mater. 49 (1) (2001) 21–29.
[30] C. Xu, M. Furukawa, Z. Horita, T.G. Langdon, Using ECAP to achieve grain refinement, precipitate fragmentation and high strain rate superplasticity in a spray-cast aluminum alloy, Acta Mater. 51 (20) (2003) 6139–6149.
[31] C. Xu, M. Furukawa, Z. Horita, T.G. Langdon, Influence of ECAP on precipitate distributions in a spray-cast aluminum alloy, Acta Mater. 53 (3) (2005) 749–758.
[32] J.H. Driver, Stability of nanostructured metals and alloys, Scripta Mater. 51 (8) (2004) 819–823.
[33] L.J. Zheng, H.X. Li, M.F. Hashmi, C.Q. Chen, Y. Zhang, M.G. Zeng, Evolution of microstructure and strengthening of 7050 Al alloy by ECAP combined with heat-treatment, J. Mater. Process. Technol. 171 (2006) 100–107.
[34] L.J. Zheng, C.Q. Chen, T.T. Zhou, P.Y. Liu, M.G. Zeng, Structure and properties of ultrafine-grained Al-Zn-Mg-Cu and Al-Cu-Mg-Mn alloys fabricated by ECA pressing combined with thermal treatment, Mater. Char. 49 (2003) 455–461.
[35] K.R. Cardoso, D.N. Travessa, W.J. Botta, A.M. Jorge Junior, High Strength AA7050 Al alloy processed by ECAP: microstructure and mechanical properties, Mater. Sci. Eng. 528 (18) (2011) 5804–5811.
[36] T. Gundu, L. Tuleun, O. Injor, Effect of pocket die bearing geometry on direct cold extrusion process responses, Am. J. Mech. Eng. 2 (3) (2014) 65–69.
[37] G. Sha, Y.B. Wang, X.Z. Liao, Z.C. Duan, S.P. Ringer, T.G. Langdon, Influence of equal-Channel Angular pressing on precipitation in an Al-Zn-Mg-Cu alloy, Acta Mater. 57 (2009) 3123–3132.
[38] A. Gholinia, P.B. Prangnell, M.V. Markushev, The effect of strain path on the development of deformation structures in severely deformed aluminum alloys processed by ECAE, Acta Mater. 48 (2000) 1115–1130.
[39] P.B. Prangnell, J.R. Bowen, P.J. Apps, Ultra-fine grain structure in aluminum alloys by severe deformation processing, Mater. Sci. Eng. (2004) 178–185, 375-377.
[40] S. Zhang, W. Hu, R. Berghammer, G. Gottstein, Microstructure evolution and deformation behaviour of ultrafine-grained Al-Zn-Mg alloys with fine η' precipitates, Acta Mater. 58 (20) (2010) 6695–6705.

[41] K.R. Cardoso, D.N. Travessa, W.J. Botta, A.M. Jorge Jr., High strength AA7050 Al alloy processed by ECAP: microstructure and mechanical properties, Mater. Sci. Eng. 528 (18) (2011) 5804–5811.
[42] Y.H. Zhao, X.Z. Liao, Z. Jin, R.Z. Valiev, Y.T. Zhu, Microstructures and mechanical properties of ultrafine grained 7075 Al alloy processed by ECAP and their evolutions during annealing, Acta Mater. 52 (15) (2004) 4589–4599.
[43] N.Q. Chinh, J. Gubicza, T. Czeppe, J. Lendvai, C. Xu, R.Z. Valiev, T.G. Langdon, Developing a strategy for the processing of age hardenable alloys by ECAP at room temperature, Mater. Sci. Eng. 516 (1–2) (2009) 248–252.
[44] J. Gubicza, I. Schiller, N.Q. Chinh, J. Illy, Z. Horita, T.G. Langdon, The effect of severe plastic deformation on precipitation in supersaturated Al-Zn-Mg alloys, Mater. Sci. Eng. (2007) 77–85, 460-461.
[45] P.J. Apps, J.R. Bowen, P.B. Prangnell, The effect of coarse second-phase particles on the rate of grain refinement during severe deformation processing, Acta Mater. 51 (2003) 2811–2822.
[46] J. Xing, H. Soda, X. Yang, H. Miura, T. Sakai, Ultra-fine grain development in an AZ31 magnesium alloy during multi-directional forging under decreasing temperature conditions, J. Jpn. Inst. Light Metals 46 (2005) 1646–1650.